FLUORESCENCE ENERGY TRANSFER IN TWO DIMENSIONS

A Numeric Solution for Random and Nonrandom Distributions

BRIAN SNYDER
Department of Biochemistry, University of Virginia School of Medicine, Charlottesville, Virginia 22908

ERNESTO FREIRE
Department of Biochemistry, University of Tennessee, Knoxville, Tennessee 37916

ABSTRACT A method of Monte Carlo calculations has been applied to the problem of fluorescence energy transfer in two dimensions in order to provide a quantitative measure of the effects of nonideal mixing of lipid and protein molecules on the quenching profiles of membrane systems. These numerical techniques permit the formulation of a detailed set of equations that describes in a precise manner the quenching and depolarization properties of planar donor-acceptor distributions as a function of specific spectroscopic and organizational parameters. Because of the exact nature of the present numeric method, these results are used to evaluate critically the validity of previous approximate treatments existing in the literature. This method is also used to examine the effects of excluded volume interactions and distinct lattice structures on the expected transfer efficiencies. As a specific application, representative quenching profiles for protein-lipid mixtures, in which donor groups are covalently linked to the protein molecules and acceptor species are randomly distributed within lipid domains, have been obtained. It is found that the existence of phase-separated protein domains gives rise to a shielding effect that significantly decreases the transfer efficiencies with respect to those expected for an ideal distribution of protein molecules. The results from the present numerical study indicate that the experimental application of fluorescence energy transfer measurements in multicomponent membrane systems can be used to obtain organizational parameters that accurately reflect the lateral distribution of protein and lipid molecules within the bilayer membrane.

INTRODUCTION

The "resonance" transfer of radiative energy between excitable dye molecules has long been recognized as a unique physical process that can provide information regarding the magnitude of interspecies separation distances within a fluorescent system (1). Applications of fluorescence energy transfer in biological systems are twofold: (*a*) measurement of unique sets of intra- or intermolecular separations (2–4), and (*b*) characterization of statistical ensembles of separation distances between donor and acceptor groups (5–8). A special case, hereafter called cqfp (concentration quenching of fluorescence polarization), arises when the incident radiation is polarized in at least one direction of observation. Here, even in the absence of translational and rotational molecular dynamics, a depolarization of the emergent radiation can occur if the transition dipoles of the fluorescent ensemble are randomly oriented with respect to the initially excited fluorophore molecules (9). This technique has been used to measure fluorescence properties and ligand distributions for various serum proteins (10, 11) and to determine organizational properties of fluorescent lipid probes (A. M. Kleinfeld, personal communication), cholesterol analogues (7) and intramembraneous proteins (12, 13) within lipid bilayers. Even though cqfp and standard intensity quenching are very sensitive to the actual distribution of fluorescent species, their application to the study of molecular organization has been limited by the fact that only approximate mathematical solutions exist in the literature and that a general treatment of nonideality has previously been unavailable (9, 14–20). Nowadays, this situation can be alleviated by the widespread availability of fast computers with large storage capacities.

Recently, we have developed a method of Monte Carlo calculations that circumvents the problems inherent in an analytic treatment of nonideality by directly simulating the mixing process with the aid of a computer (21). The error involved in a numeric analysis of this kind is determined solely by the accuracy of the representation model and the amount of computing time invested. In other words, the

Dr. Snyder's present address is the Department of Chemistry, Cornell University, Ithaca, NY 14853.

treatment is exact except for random statistical errors that can be made negligible through successive time or ensemble averaging. So far, the above method has been applied to binary-lipid, cholesterol-lipid, and protein-lipid systems such that the lateral distribution of molecules within the mixture can be obtained as a function of the molecular cross-sectional areas, mole fractions, and interaction energies between components (22–24). These computer experiments provide a complete set of position coordinates for the molecular ensemble that reflects the energetics of the mixing process in a precise manner. Thus, any thermodynamic or spectroscopic quantity that is dependent on the intermolecular distances between component molecules can be directly evaluated as a function of the mixing parameters with no underlying procedural assumptions.

In this communication, the above theoretical treatment is utilized to provide an exact yet generalized numeric solution for the concentration dependence of fluorescence quenching and depolarization in two dimensions. Concentration profiles for both random and nonrandom planar fluorophore distributions are presented. In addition, the effects of specific lattice structures and excluded volume interactions on the expected transfer efficiencies are examined. These results are used to assess the validity of the previously existing analytical theories. Finally, a critical evaluation of the range of validity of this technique with respect to the study of membrane organization and intramembraneous species distributions is presented. Empirical curve fittings of the concentration profiles are presented to facilitate the analysis of experimental quenching and depolarization curves and to permit the transformation of spectroscopic data into specific organizational parameters of the membrane.

THEORY

According to Förster's resonance theory of nonradiative energy transfer, the rate of excitation exchange between a donor j and an acceptor k is given by (14)

$$F_{jk} = \tau_o^{-1}(R_o/R_{jk})^6 \tag{1}$$

where τ_o is the intrinsic radiative decay lifetime for the donor, R_o is the distance of half transfer efficiency, and R_{jk} is the separation distance between the donor and acceptor molecules. For convenience, F_{jk} is normally expressed in terms of the observed fluorescence lifetime of the donor, τ, such that

$$F_{jk} = \tau^{-1}(\bar{R}_o/R_{jk})^6 \tag{2}$$

where

$$\bar{R}_o = Q_D^{1/6} R_o \tag{3}$$

and Q_D is the observed fluorescence quantum yield of the donor in the absence of acceptor (20). In principle, Q_D, τ, and R_o are all experimentally obtainable quantities; however, R_o determinations require some knowledge regarding the relative dipole orientations of the donor and acceptor excitons (6, 25). Normally, these orientations are considered to be isotropic with dynamic averaging over the lifetime of the donor excitation. For membrane systems, this approximation induces a maximum error of ±10% in the calculated value of $\bar{R}_o$ (6).

To apply Eq. 2 to a planar ensemble of fluorescent molecules, the following assumptions on the nature of the fluorescent system are required: (*a*) the number of excited species is low enough that their steady-state concentration is small when compared with the total concentration of fluorophores; (*b*) R_o is independent of the particular donor-acceptor pair, their separation, and radial orientation; and (*c*) the distribution of fluorescent species can be considered as static or dynamically averaged over the lifetime of the donor excitation. These conditions are equivalent to assuming an isotropic transfer rate with the entire pool of fluorophores available for transfer. The reciprocal motion of excitation within the molecular ensemble can then be described in terms of a coupled system of differential equations of the form (9)

$$\frac{\partial \rho_j}{\partial t}(t) = -\frac{\rho_j}{\tau}(t) + \sum_{k \neq j}^{N} F_{kj}\,[\rho_k(t) - \rho_j(t)] \tag{4}$$

where the sum k is over all fluorescent molecules and $\rho_j(t)$ is the probability that fluorophore j is excited at a time t after excitation. Note that these equations include both rate energy is transferred to, in addition to the rate energy leaves the initially excited molecule. In donor-acceptor fluorophore systems in which excitation quenched by an acceptor species cannot be transferred back to the initially excited molecule, the $F_{jk}\rho_k(t)$ term can be neglected and Eq. 4 becomes uncoupled (14). This is the situation encountered in quenching of fluorescence intensity by energy transfer. For this latter case, analytic solutions have previously been obtained for random distributions of fluorophores (19, 20).

For unidirectional quenching, integrating Eq. 4 under the boundary conditions $\rho_j(0) = 1$ and $\rho_j(\infty) = 0$ one obtains

$$\rho_j(t) = \exp\left[-\left(\tau^{-1} + \sum_{k-1}^{N_A} F_{jk}\right)t\right]. \tag{5}$$

The quantity of interest is obtained after integration over the lifetime

$$\bar{\rho}_j = \tau^{-1}\int_0^\infty \rho_j(t)\,dt \tag{6}$$

and is equal to the time-independent probability that the fluorescent radiation is emitted by the initially excited molecule (9, 17). Performing the integration and substituting for F_{jk} yields

$$\bar{\rho}_j = \left[1 + \sum_{k-1}^{N_A} (\bar{R}_o/R_{jk})^6\right]^{-1}. \tag{7}$$

It follows that for intensity quenching the ensemble average for the ratio of the quantum yield in the presence and absence of acceptors Q_{DA}/Q_D, is given by

$$Q_{DA}/Q_D = \frac{1}{N_D}\sum_{j-1}^{N_D} \bar{\rho}_j = \frac{1}{N_D}\sum_{j-1}^{N_D}\left[1 + \sum_{k-1}^{N_A} (\bar{R}_o/R_{jk})^6\right]^{-1} \tag{8}$$

where the sum j is over all donors.

For cqfp the coupled nature of Eq. 4 has precluded an exact analytical solution even for the random case. However, an explicit expression for $\bar{\rho}_j$ in terms of the individual rates of transfer can be obtained using a standard matrix approach (26, 27). By defining

$$G_{jk} = F_{jk}(1 - \delta_{jk}) + \left(\tau^{-1} + \sum_{m \neq j}^{N} F_{jm}\right)\delta_{jk} \tag{9}$$

where δ_{jk} is the Kronecker delta function

$$\delta_{jk} = \begin{cases} 0; j \neq k \\ 1; j = k. \end{cases} \tag{10}$$

The system of equations defined by Eq. 4 can be transformed into

$$\frac{\partial \rho_j}{\partial t}(t) = -\sum_{k-1}^{N} G_{jk}\,\rho_k(t). \tag{11}$$

This equation is easily solved for $\rho_j(t)$ by taking the inverse of the transfer matrix $|G|$ such that

$$\rho_j(t) = \sum_{k-1}^{N} (G^{-1})_{jk} \cdot \frac{\partial \rho_k}{\partial t}(t). \tag{12}$$

The integrated solution to the above equation for the given boundary conditions is (17)

$$\bar{\rho}_j = \tau^{-1} (G^{-1})_{jj}. \tag{13}$$

It follows that the ensemble average of $\bar{\rho}_j$ for a system of N fluorophores is given by

$$\langle \bar{\rho} \rangle = \frac{1}{N} \sum_{j-1}^{N} \bar{\rho}_j = \frac{1}{\tau N} Tr(G^{-1}). \tag{14}$$

The quantity obtained experimentally is the degree of polarization, p, defined in terms of the fluorescence intensities in directions parallel and perpendicular to the incident radiation by

$$p = \frac{I_\parallel - I_\perp}{I_\parallel + I_\perp}. \tag{15}$$

The polarization function, $g(p)$, is defined as

$$g(p) = \left(\frac{1}{p} - \frac{1}{3}\right)^{-1}. \tag{16}$$

This quantity is related to $\langle \bar{\rho} \rangle$ by (9)

$$g(p)/g(p_o) = \langle \bar{\rho} \rangle \tag{17}$$

where p_o is the infinite dilution limit of p.

The analytic treatments presented above illustrate that within the framework of the Förster mechanism, expected quenching and depolarization efficiencies within a fluorescent ensemble can be obtained if the set of separation distances between donor and acceptor excitons is known. In previous communications (21–24), we have developed a method for computer-generating lateral distributions of molecules in binary mixtures of lipids, cholesterol-lipid, and protein-lipid systems. This computer method provides a precise set of position coordinates from which intermolecular distances may be calculated as a function of the interaction energies between component species and their relative concentrations. Interaction energies are expressed in terms of a single parameter P, a Boltzmann exponent $\alpha \exp(\Delta E_m/kT)$, where ΔE_m is the excess energy of mixing. A P value of 1 defines the ideal mixture where the two components are distributed randomly within the bilayer matrix. A $P > 1$ reflects the tendency for individual components to undergo self-aggregation into compositionally distinct domains. Conversely, $P < 1$ corresponds to the case where contact between like species is unfavorable and domain size approaches a minimum. The magnitude of P determines the degree of species aggregation or repulsion. Typical computer generated distributions for various P values are shown in Fig. 1. Detailed analyses of these distributions are presented in references 21 and 22.

In the present work, the above Monte Carlo techniques are utilized for the purpose of directly tabulating fluorophore separation distances as a function of the mixing parameter P. Molecular distributions are calculated for two different planar arrangements: (*a*) a hexagonal case where component molecules are constrained to occupy sites on a triangular lattice and (*b*) a continuous case where component molecules are allowed to "float" on a two-dimensional surface. For the triangular lattice, the distance, R, between any two molecules located on lattice sites (i, j) and (i', j') is given by (24)

$$R = \sqrt{X^2 + Y^2} \tag{18}$$

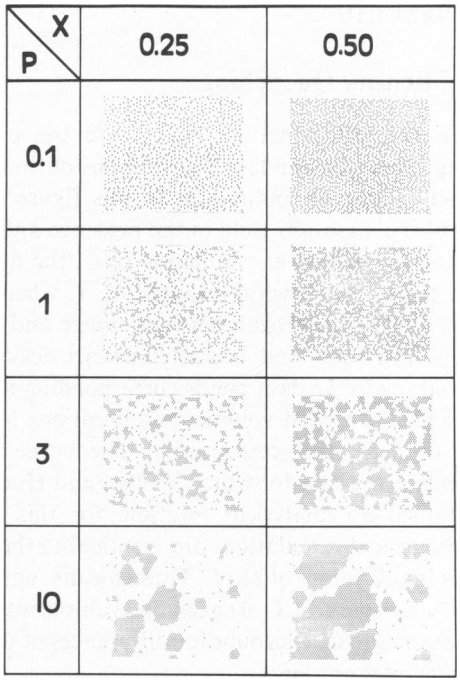

FIGURE 1 Typical computer generated distributions of two-component bilayer mixtures for P values of 0.1, 1, 3, and 10 and mole fractions of 0.25 and 0.50. These distributions were obtained using periodic 62 × 62 triangular lipid lattices.

where

$$Y = |i' - i| \frac{\sqrt{3}}{2} d \tag{19}$$

$$X = \left[|j' - j| + \frac{1}{2} \operatorname{sgn}(j' - j) \epsilon_{i',i} \right] d \tag{20}$$

d is the lattice spacing between coordinate positions and $\epsilon_{i',i}$ is parity symbol defined as

$$\epsilon_{i',i} \begin{cases} 0; & P_i = P_{i'} \\ +1; & i' \text{ even}, i \text{ odd} \\ -1; & i' \text{ odd}, i \text{ even}. \end{cases} \tag{21}$$

For the continuous case, the distance, R, between any two molecules with coordinates (i, j) and (i', j') is given simply by

$$R = \sqrt{|i' - i|^2 + |j' - j|^2}\, d. \tag{22}$$

Through the direct application of Eqs. 8 and 17, the Monte Carlo techniques described above permit the calculation of precise Q_{DA}/Q_D and $g(p)/g(p_o)$ ratios as a function of $\bar{R}_o$, the concentration of fluorescent species and their lateral distribution within planar membrane systems. As such, these techniques provide a unique method for obtaining a quantitative estimate for the effects of spatial organization, domain structure and the physical state of the lipid bilayer on the quenching and depolarization characteristics of membrane and model membrane systems.

RESULTS

Intensity Quenching

Shown in the left panel of Fig. 2 are the calculated quenching curves for random distributions of fluorophores in a two-dimensional continuum. In this figure Q_{DA}/Q_D, the ratio of the quantum yield in the presence and absence of acceptors, is plotted as a function of C, the number of acceptors per $\bar{R}_o^2$, for several values of $\bar{R}_o/L$, where L is the distance of closest approach between donor and acceptor molecules. The solid and broken lines are least-squares exponential fits to the data points corresponding to simulations in which excluded volume considerations have been included or neglected, respectively. The latter situation corresponds to the case for which Wolber and Hudson (19) have obtained an analytical solution; for this case the present numerical calculations are identical to the analytical values for all values of $\bar{R}_o/L$. These results indicate that for small values of $\bar{R}_o/L$ (<4) excluded volume interactions are important and can account for differences of up to 20% in the quenching profiles.

For all cases, single exponential functions of the form

$$Q_{DA}/Q_D = \exp\,[B(\bar{R}_o/L)\cdot C] \tag{23}$$

provided an excellent representation of the quenching curves for all values of $\bar{R}_o/L$. The decay constants $B(\bar{R}_o/L)$ were found to be smooth functions of $\bar{R}_o/L$ and could be fit

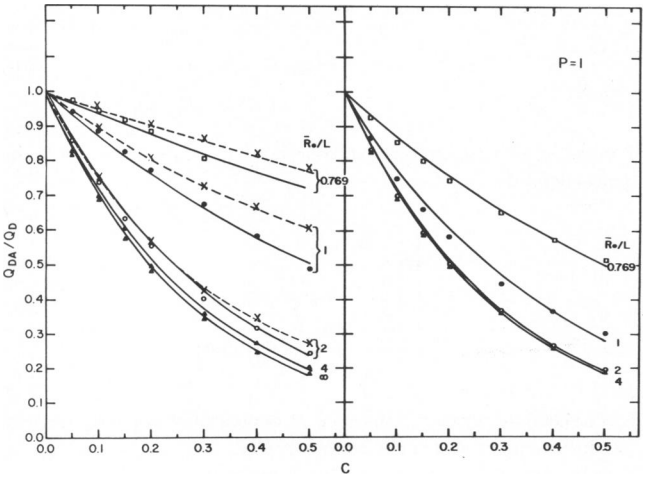

FIGURE 2 Calculated quenching curves for random distributions of fluorophores in a two-dimensional continuum (left panel) and triangular lattice (right panel). Shown are plots of Q_{DA}/Q_D, the ratio of the quantum yield in the presence and absence of acceptors, as a function of C, the number of acceptors per $\bar{R}_o^2$, for $\bar{R}_o/L$ values of 0.769 (□), 1 (●), 2 (○), 4 (▲) and ∞ (△). The × represent data points calculated neglecting excluded volume considerations. The solid (—) and broken lines (---) are least-squares exponential fits corresponding to the simulations in which excluded volume considerations have been included or neglected, respectively.

to a third order polynomial of the form

$$B(\bar{R}_o/L) = \sum_{i=0}^{3}\alpha_i\,(\bar{R}_o/L)^{-i} \tag{24}$$

where

$$\alpha_0 = -3.448; \qquad \alpha_1 = -0.4021;$$
$$\alpha_2 = 4.136; \qquad \alpha_3 = -1.668.$$

The results for the case where fluorophore molecules are constrained to occupy sites on a two-dimensional triangular lattice are presented on the right panel of Fig. 2. Except for the planar arrangement, conditions are identical to that of the continuum case. For low values of $\bar{R}_o/L$, these quenching profiles reflect an increased degree of transfer efficiency over the continuum case. For $\bar{R}_o/L$ values >2 quenching profiles for the lattice and continuum cases are the same within statistical error. Numerical fitting of the quenching profiles in terms of Eqs. 23 and 24 yields

$$\alpha_0 = -3.238, \qquad \alpha_1 = -0.7508,$$
$$\alpha_2 = 0.8824, \qquad \alpha_3 = 0.6149,$$

for the overall $Q_{DA}/Q_D(\bar{R}_o/L,C)$ representation of the lattice case.

For nonrandom distributions of fluorophores ($P > 1$), Q_{DA}/Q_D values were plotted as a function of P for constant $\bar{R}_o/L$ and probe concentrations ranging between 0.5–5.0 mol %. A typical family of curves is shown in Fig. 3. The Q_{DA}/Q_D vs. P curves were fit to exponential functions of the form Ae^{BP} and the dependence of A and B on the concentration of probes and $\bar{R}_o$ was investigated. The preexponential factor A was found to be a simple exponential function of $C = X\bar{R}_o^2$ whereas the B constants were found to be separate functions of X and $\bar{R}_o^2$, where X is the mole fraction of fluorescent probes. For $\bar{R}_o \geq 2$, and constant X, B was directly proportional to $\bar{R}_o^2$; however, for $\bar{R}_o = 1$, B was a separate empirical function of X, independent of $\bar{R}_o$. For simplicity, in what follows L has been normalized to 1 so that $\bar{R}_o/L = \bar{R}_o$. The plots of A vs. C and B vs. $\bar{R}_o^2$ are shown in Fig. 4. To obtain an overall representation of Q_{DA}/Q_D as a function of P, X, and $\bar{R}_o$, both the slope/intercept constants of the B vs. $\bar{R}_o^2$ curves for $\bar{R}_o \geq 2$ and the B constants for $\bar{R}_o = 1$ were fit to quadratic functions of X to yield an equation of the form

$$Q_{DA}/Q_D\,(P,X,\bar{R}_o) = A(C)\,\exp\,[B(X,\bar{R}_o)\cdot P] \tag{25}$$

where

$$A(C) = 1.036\,\exp\,[-3.392C] \tag{26}$$

and

$$B(X,\bar{R}_o) = \begin{cases} 5.987\times10^{-5} - 3.619X + 34.88X^2; \bar{R}_o = 1 \\ B_1(X)\bar{R}_o^2 + B_2(X); \bar{R}_o \geq 2 \end{cases} \tag{27}$$

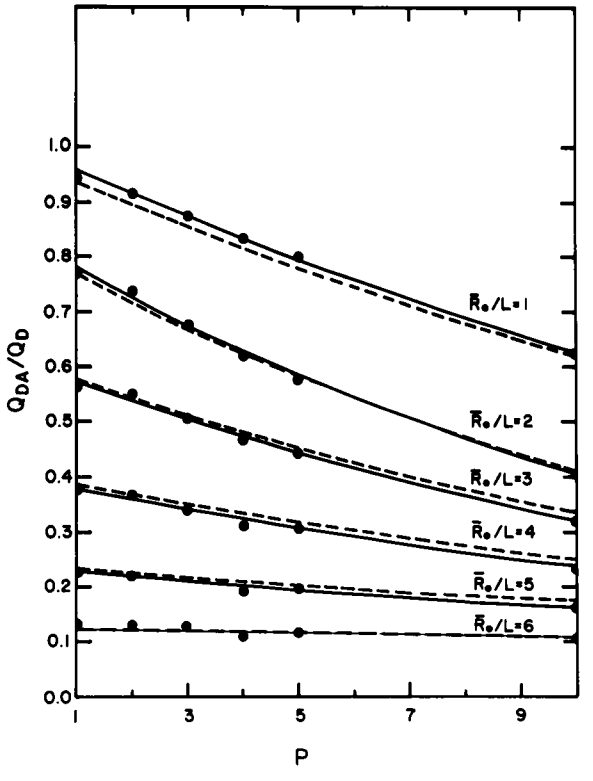

FIGURE 3 Calculated Q_{DA}/Q_D values as a function of the affinity constant P for several values of $\bar{R}_o/L$ with a probe mole fraction of 0.015. The solid lines (—) represent the original least-squares exponential fits to the data points whereas the broken curves (---) represent the reconstituted curves obtained using Eqs. 25–29.

where

$$B_1(X) = -6.211 \times 10^{-4} + 0.1168X + 2.922X^2 \quad (28)$$

$$B_2(X) = -3.826 \times 10^{-3} - 5.378X + 37.28X^2. \quad (29)$$

The use of Eq. 25 in conjunction with Eqs. 26–29 allows one to calculate the expected quenching curves for any value of P, $\bar{R}_o$, and concentration of fluorescent probes. Typical numeric results with the original Q_{DA}/Q_D vs. P exponential fits and the reconstituted curves using the above representation method are shown in Fig. 3 for X = 0.015. This representation is good to within 4% of the original curves.

In Fig. 5 are shown plots of Q_{DA}/Q_D vs. C at three different values of P for probe mole fractions ranging from 0.005–0.050. For P = 1 all data points lie on a single exponential curve indicating that the probability for excitation transfer is independent of the value of $\bar{R}_o/L$ for these probe mole fractions and distribution ensembles. This is due to the fact that at these very low probe concentrations, the probability of molecular contact between randomly distributed probe molecules is so negligible that the quenching profiles are independent of L, the distance of

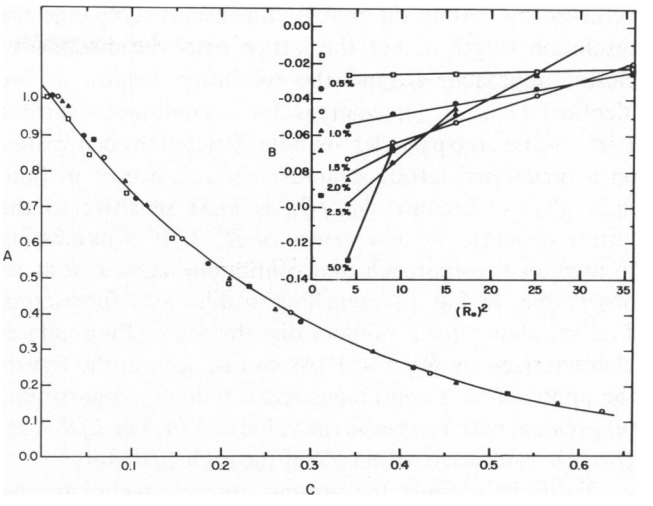

FIGURE 4 Dependence of the preexponential factor A on the normalized acceptor concentration C for probe mole fractions of 0.005 (□), 0.010 (●), 0.015 (○), 0.020 (▲), 0.025 (△), and 0.050 (■). Inset, dependence of decay constants B on $\bar{R}_o^2$ for similar probe mole fractions.

closest approach, and depend solely on the number of possible acceptors within the reaction radius of $\bar{R}_o$. For higher P values (3 and 10) the attractive potential increases the probability of molecular contacts such that the quenching efficiency exhibits an increased dependence on the value of L and hence $\bar{R}_o/L$. These arguments also explain why the exponential constants A, the limiting values of the quenching ratio for infinitely repulsive nearest neighbor interactions, depend only on the value of C.

Recently, we have developed a generalized matrix representation that allows generation of both random and nonrandom particle distributions in quasi-continuous two-dimensional surfaces (24). The approach to a continuum is

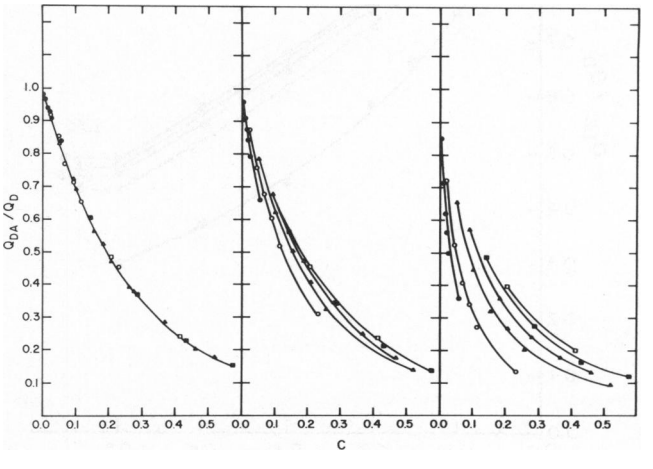

FIGURE 5 Calculated Q_{DA}/Q_D values as a function of the normalized acceptor concentration C for probe mole fractions <0.050 and $\bar{R}_o/L$ ratios of 1 (●), 2 (○), 3 (▲), 4 (△), 5 (■), and 6 (□). Shown are the results for three values of the affinity constant P: 1 (left panel), 3 (center panel), and 10 (right panel).

achieved by scaling the matrix dimensions to change the resolution length d. For the lattice case, the distance of closest approach, L, and the resolution length, d, are identical ($L/d = 1$); whereas for a continuous surface $L/d = \infty$, i.e., the particles are not restricted to occupy sites on a predefined lattice structure such as occurs in fluid lipid phases. Because Q_{DA}/Q_D is most sensitive to the lattice structure for low values of $\bar{R}_o/L$, it is interesting to monitor the approach to a continuum using L/d as an observable. In Fig. 6, quenching profiles as a function of L/d are shown for a random distribution of fluorophores characterized by $\bar{R}_o/L = 1$. As can be seen in the figure, the approach to a continuous space follows a logarithmic progression with respect to the value of L/d. For $L/d = 25$, Q_{DA}/Q_D values are within 5% of the high L/d limit.

To directly apply the present numeric technique, we have calculated the expected quenching profiles of protein-lipid mixtures in which the donor groups are covalently linked to the protein molecules and the acceptor molecules are randomly distributed within the bilayer. In this case, computer experiments are initialized by distributing protein molecules in a lipid bilayer matrix with a given value of P (see reference 24 for details) with donor fluorophores attached to specific sites on the protein molecules. Subsequently a selected number of acceptor fluorophores are randomly distributed within the residual lipid domains, donor-acceptor separation distances are measured and Q_{DA}/Q_D is calculated following Eq. 8.

Presented in Fig. 7 are the calculated quenching profiles for protein-lipid mixtures in which the donor groups are located at the protein centers of mass. To mimic the experimental situation, the quenching ratios have been plotted as a function of the fraction of labeled lipid molecules. Shown in the top half of the figure are the results for the case in which the cross-sectional areas of the protein and lipid molecules are the same. Presented in the bottom half of the figure are the results for an R_P/R_L value of 3 where R_P/R_L is the ratio of protein-to-lipid cross-sectional radii. It should be noted that the simulations for the case where $R_P/R_L = 1$ are also representative of a binary lipid mixture in which the donor and acceptor species are constrained to occupy sites within respective

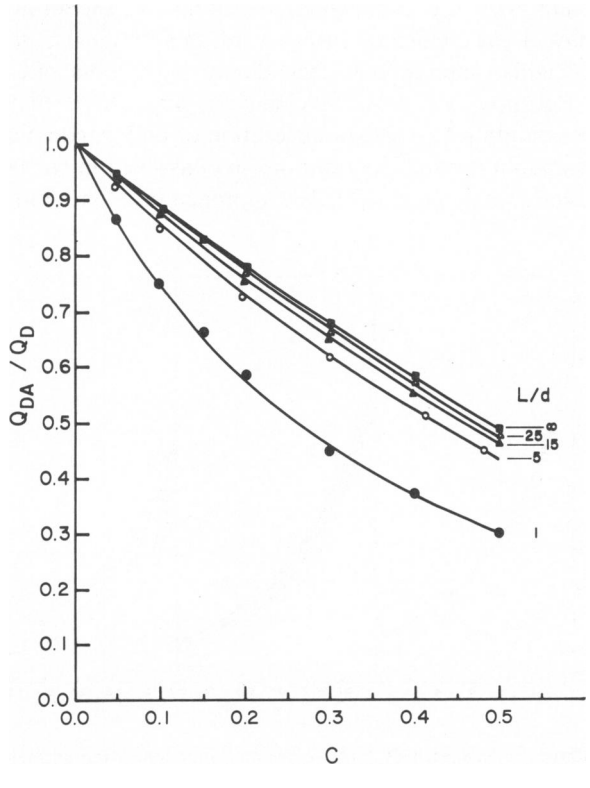

FIGURE 6 Calculated quenching profiles for a random distribution of fluorophores and L/d resolution ratios of 1 (●), 5 (○), 15 (▲), 25 (△), and ∞ (■) where $\bar{R}_o/L = 1$ and $P = 1$.

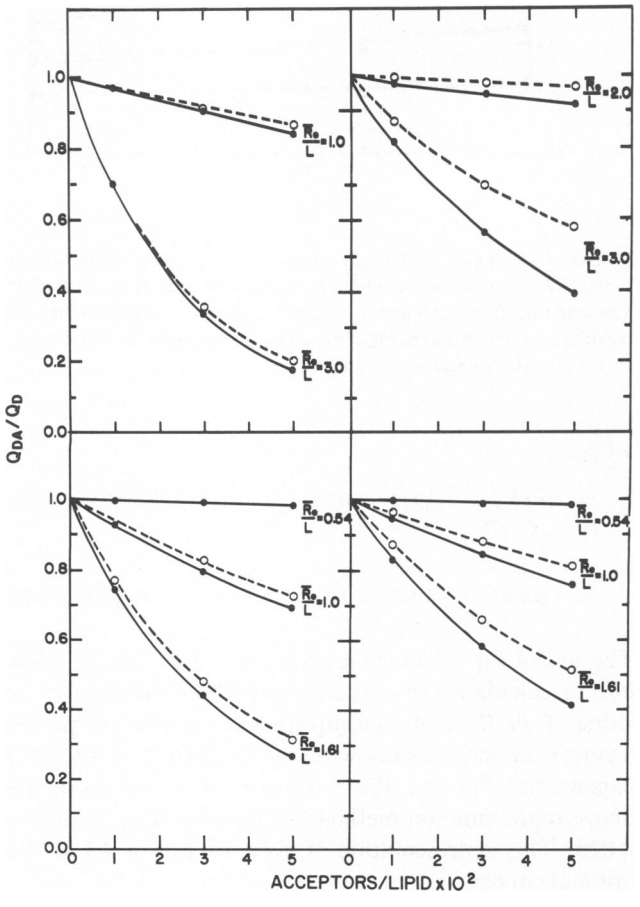

FIGURE 7 Calculated quenching profiles for protein-lipid systems in which the donor moiety is located at sites corresponding to individual protein centers of mass. Shown are plots Q_{DA}/Q_D as a function of ACCEPTORS/LIPID, the fraction of labeled lipid molecules, for several values of $\bar{R}_o/L$. Presented in the top and bottom halves of the figure, respectively, are the results for R_P/R_L values of 1 and 3 where R_P/R_L is the ratio of protein-to-lipid radii. Calculated transfer efficiencies for protein-to-lipid mole ratios (prot/lip) of 0.020 and P values of 1 (●,—) and 5 (○,---) are shown on the left two panels. Similar calculations for prot/lip values of 0.500 for $R_P/R_L = 1$ and 0.144 for $R_P/R_L = 3$ are shown in the right two panels.

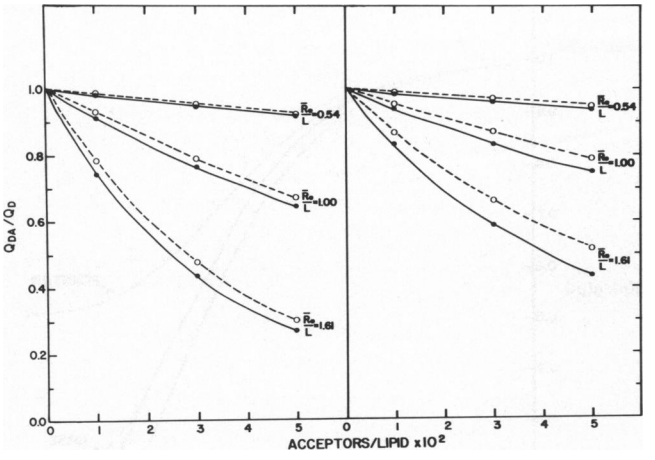

FIGURE 8 Calculated quenching profiles for protein-lipid systems characterized by an off-center donor positioning and an R_P/R_L value of 3. Here each donor fluorophore is located at a distance 2/3 R_P from the protein centers of mass with a random angular orientation. Shown are plots of Q_{DA}/Q_D vs. ACCEPTORS/LIPID for several values of $\overline{R}_o/L$. Presented in the left panel are the results for a prot/lip ratio of 0.020 and P values of 1 (●,—) and 5 (○,---). Similar calculations for a prot/lip ratio of 0.144 are presented in the right panel.

compositional domains. Calculated transfer efficiencies for protein-to-lipid mole ratios (prot/lip) of 0.020 are shown in the left two panels of the figure. Similar calculations for prot/lip values of 0.500 for $R_P/R_L = 1$ and 0.144 for $R_P/R_L = 3$ shown in the right two panels. These latter quenching profiles correspond to the percolation threshhold concentrations (24) where ~50% of the membrane surface is occupied by the protein species. In each panel, quenching profiles are presented for a particular set of $\overline{R}_o/L$ values dependent on the value of R_P/R_L. Here, L is the distance of closest approach between protein and lipid centers of mass.

For each group of R_P/R_L, prot/lip, and $\overline{R}_o/L$ values, two types of quenching curves are presented; first, a $P = 1$ case (solid curves) where, except for a hard core potential, protein molecules are distributed neglecting specific protein-protein interactions and second, a $P = 5$ case (broken curves) where the distribution of protein molecules is characterized by significant amounts of lateral species separation. As can be seen in the figure, two general properties of organizational effects on quenching characteristics in protein-lipid systems can be deduced: (*a*) an increase in the value of P decreases the relative amounts of fluorescence quenching and (*b*) as the value of either $\overline{R}_o/L$ or prot/lip is increased the P effects are enhanced. These organizational effects can be interpreted in terms of the shielding properties relating to the degree of ramification and compactness, respectively, of random and phase-separated lateral distributions (22). For P values of 1, the relative distribution of the protein component along the plane of the bilayer gives rise to highly ramified compositional domains such that each protein molecule is close to a relatively large number of lipid molecules and hence possible acceptor positions. As the value of P increase, the domains become more compact isolating greater fractions of the protein molecules from the lipid matrix and therefore shielding the donor fluorophores from the quenching species. For higher prot/lip and $\overline{R}_o/L$ ratios the relative shielding effects are increased due to the larger number of protein molecules involved in the compactness process.

Similar quenching profiles for protein-lipid systems characterized by an off-center donor positioning and an R_P/R_L value of 3 are presented in Fig. 8. Here each donor fluorophore is located at a distance 2/3 R_P from the protein centers of mass with a random angular orientation. For $\overline{R}_o/L \geq 1$, the resulting quenching profiles for both values of P exhibit a slight increase in transfer efficiency with respect to those calculated for the case in which donors are placed at the protein centers of mass. This increase in quenching efficiency is due to a decrease in the allowed distance of closest approach between donor and acceptor species due to the radial positioning of the donor fluorophore. For $\overline{R}_o > 1$, where minimum separations are less important, the resulting quenching profiles are identical, within statistical error, for both types of donor placements. It should be noted that although the absolute quenching ratios may vary, the relative P effects for all values of $\overline{R}_o/L$ are equivalent.

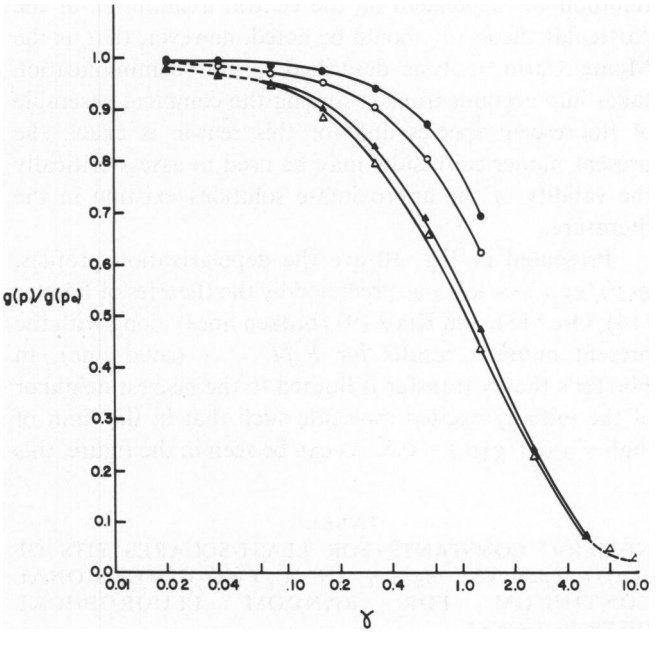

FIGURE 9 Calculated depolarization in a two-dimensional continuum for random fluorophore distributions and various excluded volume interactions. Shown are plots of the depolarization ratio, $g(p)/g(p_\infty)$, as a function of the log of the normalized fluorophore concentration, γ, for $\overline{R}_o/L$ values of 0.769 (●), 1 (○), 2 (▲), and ≥ 4 (△). The solid curves are the least-squares fits presented in Table I over the range in which the fitting procedure provides an accurate representation of the depolarization data.

Transfer Depolarization

Shown in Fig. 9 are the calculated depolarization profiles for random distributions of fluorophores in a two-dimensional continuum. In this figure, $g(p)/g(p_o)$ is plotted as function of log γ for several values of $\bar{R}_o/L$, where γ is the number concentration of acceptors per $\pi \bar{R}_o^2$ and L is the distance of closest approach between fluorescent species. The accompanying curves are fourth degree polynomial least-squares fits of the data vs. log γ with the solid portions corresponding to the ranges of validity of the fitting procedure. The numerical constants for the various powers of log γ and $\bar{R}_o/L$ values are presented in Table I. As can be seen in the Fig. 9, for constant γ, increasing the value of $\bar{R}_o/L$ increases the relative amounts of depolarization until a limiting $g(p)/g(p_o)$ value is reached at $\bar{R}_o/L \simeq 4$. At this point, the degree of quenching is no longer dependent on the distance of closest approach but is solely a function of the normalized concentration of fluorophores. These results are qualitatively similar to those described above for fluorescent systems in which no back transfer can occur.

Previously, analytic theories for the concentration dependence of $g(p)/g(p_o)$ have been limited to the special case in which excluded volume interactions between fluorophore molecules are neglected, i.e., $\bar{R}_o/L = \infty$. These treatments have all been approximate in the sense that transfer was restricted to only a certain fraction of the fluorophores dependent on the central assumption of the particular theory. It should be noted, however, that as the Monte Carlo analysis described in this communication takes into account transfer among the complete ensemble of fluorescent species and for this reason is exact, the present numerical results may be used to assess critically the validity of the approximate solutions existing in the literature.

Presented in Fig. 10 are the depolarization profiles, $g(p)/g(p_o)$ vs. log γ as predicted by the theories of Förster (14), Ore (15), and Knox (9) (broken lines) along with the present numeric results for $\bar{R}_o/L = \infty$ (solid line). In Förster's theory transfer is limited to the nearest neighbor of the initially excited molecule such that in the limit of high γ, $g(p)/g(p_o) = 0.5$. As can be seen in the figure, this

TABLE I

NUMERIC CONSTANTS FOR LEAST-SQUARES FITS OF $g(p)/g\ (p_o)$ VS. $\log_{10}\ \gamma$ IN A TWO-DIMENSIONAL CONTINUUM FOR RANDOM FLUOROPHORE DISTRIBUTIONS*

$\bar{R}_o/L$	α_0	α_1	α_2	α_3	α_4
0.769	0.7703	−0.6401	−0.7826	−0.4512	−0.0980
1	0.6987	−0.6562	−0.6153	−0.2732	−0.0495
2	0.5477	−0.7017	−0.1800	0.2333	0.1097
4	0.5101	−0.6854	−0.1187	0.2347	0.0971

*The computer generated depolarization ratios were fit to a fourth-order polynomial of the form $g(p)/g(p_0) = \Sigma_{i=0}^{4} \alpha_i (\log_{10} \gamma)^i$.

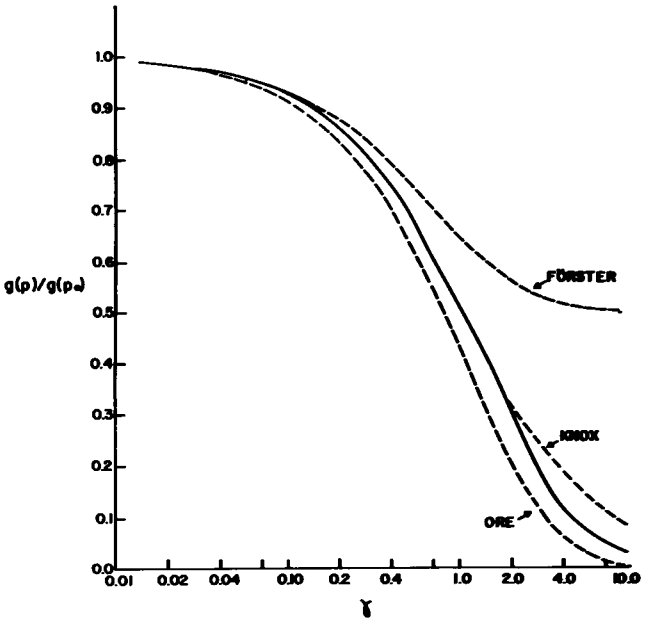

FIGURE 10 Comparison of the theories of Förster (14), Ore (15), and Knox (9) (broken curves, ---) with the present numeric results neglecting excluded volume considerations (solid curve, —). Shown are the predicted depolarization ratios $g(p)/g(p_o)$, as a function of the log of the normalized fluorophore concentration γ. $\bar{R}_o/L = \infty$.

approximation remains valid for γ values ≤ 0.1 at which point transfer to other than nearest neighbor fluorophores becomes progressively more significant. Ore's theory modifies Förster's theory to include transfer to more distant neighbors if the initially excited species is not also the nearest neighbor of its nearest neighbor species. This approximation yields closer agreement with the exact solution at high γ, yet for all γ predicts a slightly enhanced depolarization with respect to the exact values of $g(p)/g(p_o)$.

The most complete analytic treatment of cqfp, the theory of Knox (9), and Craver and Knox (17), involves the separation of the fluorescent ensemble into mutually exclusive physical clusters where all elements of a particular cluster are within $\bar{R}_o$ of at least one other cluster element and $>\bar{R}_o$ from all elements outside the cluster. The excitation is then assumed to be limited to transfer within the cluster except for transfer between individual monomers. This approximation is called the "sticking approximation." In this way, the resultant depolarization of the system can be broken down into the individual contributions of clusters of size n with the final quenching ratio being a linear combination of the $g(p)/g(p_o)$ values for each particular cluster size. The profile presented in Fig. 10 includes the contributions of all clusters of size $n \leq 20$ and is accurate to within 10^{-4} of the limiting $g(p)/g(p_o)$ ratio. Note that the sticking approximation remains valid for fluorophore concentrations up to $\gamma = 1.5$, however, it still yields elevated quenching ratios in the high concentration limit when intercluster transfer can no longer be neglected.

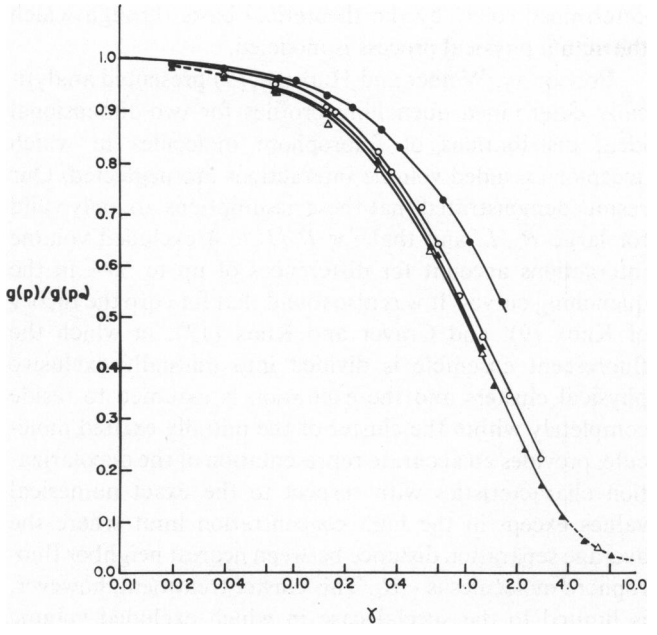

FIGURE 11 Calculated depolarization profiles in a two-dimensional triangular lattice for random fluorophore distributions (P = 1) and various excluded volume interactions. Shown are plots of the depolarization ratio, $g(p)/g(p_o)$, as a function of the log of the normalized fluorophore concentration, γ, for $\overline{R}_o/L$ values of 0.769 (●), 1 (○), 2 (▲), and ≥4 (△). The solid curves are the least-squares fits presented in Table II over the range in which the fitting procedure provides an accurate representation of the depolarization data.

The depolarization profiles for the case where fluorophore molecules are constrained to occupy sites on a two-dimensional triangular lattice are presented in Fig. 11. Except for the planar arrangement, conditions are identical to that of the continuum case, i.e., a random distribution of fluorophore molecules where P = 1. Due to the local order of the lattice system, these quenching profiles indicate an increased degree of transfer efficiency over the continuum case for low values of $\overline{R}_o/L$. In the limit of high $\overline{R}_o/L$, the quenching profiles obtained for each planar arrangement are essentially equivalent. The numerical constants of the fitting procedure for triangular case are presented in Table II. Again, these results are qualitatively similar to those found in this communication for standard donor-acceptor quenching systems.

TABLE II

NUMERIC CONSTANTS FOR LEAST-SQUARES FITS OF $g(p)/g(p_0)$ VS. LOG_{10} γ IN A TWO-DIMENSIONAL TRIANGULAR LATTICE FOR RANDOM FLUOROPHORE DISTRIBUTIONS (P = 1)*

$\overline{R}_0/L$	α_0	α_1	α_2	α_3	α_4
0.769	0.6674	−0.5491	−0.3145	−0.0528	−0.0043
1	0.5405	−0.6675	−0.1762	0.1366	0.0578
2	0.5054	−0.7147	−0.1381	0.2571	0.1113
4	0.4955	−0.6792	−0.1087	0.2219	0.0882

*The computer generated depolarization ratios were fit to a fourth-order polynomial of the form $g(p)/g(p_0) = \Sigma_{i=0}^{4} \alpha_i (\log_{10} \gamma)^i$.

To investigate the effects of aggregation among the fluorescent species, similar depolarization profiles were calculated for P values of 3, 5, and 10 for each value of $\overline{R}_o/L$. At 25°C, these P values correspond to mixing energies of 650, 950, and 1360 cal/mol, respectively and are representative of the range of P values at which the organizational parameters of lipid membranes are most sensitive to lateral phase separation phenomena (22).

Shown in Fig. 12 are plots of $g(p)/g(p_o)$ vs. log γ for P

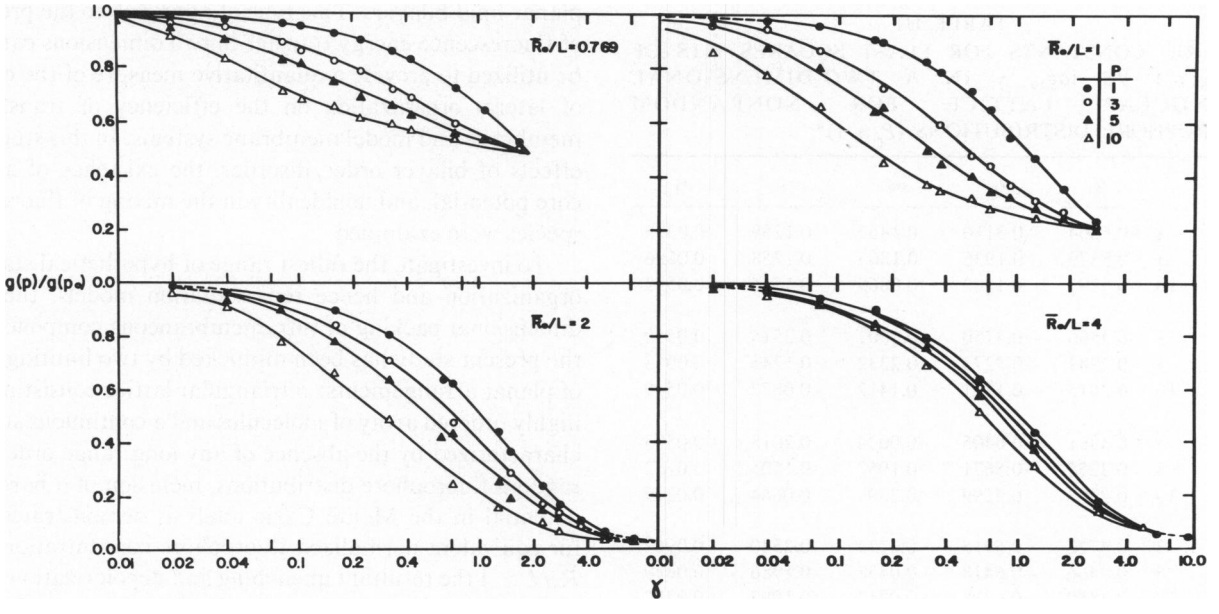

FIGURE 12 Calculated depolarization profiles in a two-dimensional triangular lattice for $\overline{R}_o/L$ ratios of 0.769, 1, 2, and 4 and P values of 1 (●), 3 (○), 5 (▲), 10 (△). Shown are plots of the depolarization ratio, $g(p)/g(p_o)$, vs. the log of the normalized fluorophore concentration γ. The solid curves are the valid portions of the least-squares fits presented in Table III.

values of 1, 3, 5, and 10 at $\bar{R}_0/L$ values of 0.769, 1, 2, and 4. For all ratios of $\bar{R}_0/L$, increasing the value of P shifts the midpoint of the depolarization profile to lower normalized concentration levels. In this figure, the limiting values of the quenching ratio in the high concentration limit, 0.50, 0.22, 0.03, and 0.02, respectively for $\bar{R}_0/L$ values of 0.769, 1, 2, and 4, reflect the maximum quenching that can occur with a planar saturation of fluorophore molecules. The numerical fitting constants for these values of P are summarized in Table III. It should be noted that the effect of lateral species aggregation on $g(p)/g(p_0)$ increases with γ until a maximum is reached in the range of $0.1 < \gamma < 1$. This maximum increases with the magnitude in the change of P and is largest for an $\bar{R}_0/L$ value of 1.

DISCUSSION

In this study, we have shown that a numerical estimate for the effect of lateral organization on the transfer of excited state energy within donor fluorescent systems can be obtained by directly simulating the mixing process with the aid of a computer. These data have been used to formulate an overall representation of expected quenching and depolarization efficiencies in terms of four parameters: $\bar{R}_0$, the experimental distance of half transfer efficiency; L, the minimum separation between donor and acceptor moieties; X, the mole fraction of the fluorescent species; and P, a Boltzmann exponent proportional to the excess energy of mixing between the fluorescent species. It should be noted that a Monte Carlo analysis of this type is exact in the sense that no mathematical assumptions or approximations are required to generate statistically precise quenching ratios. Instead, the accuracy of the simulation method is determined solely by the theoretical basis through which the actual physical process is modeled.

TABLE III

NUMERIC CONSTANTS FOR LEAST SQUARES FITS OF $g(p)/g(p_0)$ VS $\log_{10}\gamma$ IN A TWO-DIMENSIONAL TRIANGULAR LATTICE FOR NONRANDOM FLUOROPHORE DISTRIBUTIONS ($P > 1$)*

$\bar{R}_0/L$	P	α_0	α_1	α_2	α_3	α_4
	3	0.5604	−0.3110	0.1453	0.1759	0.0395
0.769	5	0.5379	−0.1935	0.1865	0.1258	0.0196
	10	0.5297	−0.1302	0.0869	−0.1846	−0.0593
	3	0.3560	−0.4750	0.2007	0.2515	0.0550
1	5	0.2987	−0.3273	0.2332	0.1245	0.0053
	10	0.2515	−0.1521	0.1412	−0.0872	−0.0549
	3	0.3991	−0.6405	−0.0034	0.2018	0.0593
2	5	0.3258	−0.5671	0.1052	0.1505	0.0132
	10	0.2097	−0.4299	0.2099	0.0664	−0.0319
	3	0.4722	−0.6915	−0.0771	0.2540	0.0967
4	5	0.4466	−0.6418	−0.0431	0.1986	0.0650
	10	0.3869	−0.6208	0.0412	0.1993	0.0473

*The computer generated depolarization ratios were fit to a fourth-order polynomial of the form $g(p)/g(p_0) = \Sigma_{i=0}^{4} \alpha_i (\log_{10}\gamma)^i$.

Previously, Wolber and Hudson (19) presented analytically determined quenching profiles for two-dimensional ideal distributions of fluorophore molecules in which acceptor excluded volume interactions are neglected. Our results demonstrated that these assumptions are only valid for large $\bar{R}_0/L$, and that for $\bar{R}_0/L < 4$ excluded volume interactions account for differences of up to 20% in the quenching curves. It was also found that for cqfp the theory of Knox (9), and Craver and Knox (17), in which the fluorescent ensemble is divided into mutually exclusive physical clusters and the excitation is assumed to reside completely within the cluster of the initially excited molecule, provides an accurate representation of the depolarization characteristics with respect to the exact numerical values except in the high concentration limit where the average separation distance between nearest neighbor fluorophore molecules is $<\bar{R}_0$. This cluster treatment, however, is limited to the special case in which excluded volume considerations and nonrandomness in the mixing of fluorophore molecules are negligible and hence, as is also the case for the theory of Wolber and Hudson (19), cannot be generalized to incorporate more complex fluorescent systems.

The formulation of an exact yet flexible numerical method as described in this communication permits the convenient calculation of precise quenching or depolarization profiles for a wide variety of organizational and spectroscopic conditions. Furthermore, the mathematical basis through which fluorophore distributions are generated and intermolecular separation distances determined has previously been used to model the two-dimensional mixing of lipid, cholesterol, and protein molecules within planar lipid bilayers. This type of approach to the problem of fluorescence energy transfer in two dimensions can thus be utilized to provide a quantitative measure of the effects of lateral organization on the efficiency of transfer in membrane and model membrane systems. In this study the effects of bilayer order/disorder, the existence of a hard core potential, and nonideality in the mixing of fluorescent species were examined.

To investigate the fullest range of hypothetical states of organization and hence representation models, the two-dimensional packing of intramembraneous components in the present study has been mimicked by two limiting types of planar arrangements: a triangular lattice consisting of a highly ordered array of molecules and a continuous surface characterized by the absence of any long range order. For random fluorophore distributions, inclusion of a hard core potential in the Monte Carlo analysis demonstrated that for equivalent normalized fluorophore concentrations and $\bar{R}_0/L \geq 4$ the resultant quenching and depolorization ratios were independent of the value of L and yielded identical concentration profiles for both types of planar arrangements. For $\bar{R}_0/L < 4$, similar profiles were shown to be a

more sensitive function of the distance of closest approach in the planar continuum and exhibited a decreased transfer efficiency with respect to the ordered triangular lattice due to the local disorder of the molecular packing. As such, these studies suggest that the local contribution of the lipid gel/liquid crystalline phase transition to the quenching or depolarization mechanism would be negligible for the case where $\overline{R}_0 >> L$ and would result in a decrease in the quenching efficiency for the case where $\overline{R}_0$ and L are approximately equivalent.

In addition to the ideal case, the quenching and depolarization of planar membrane systems containing nonrandom distributions of fluorescent species were also investigated. These distributions were characterized by increasing degrees of aggregation among the probe molecules as determined by the values of P (≤ 10) used in the generation procedure. The excess mixing energies represented by these P values correspond to the range in which the microscopic equilibrium states of the membrane are most susceptible to lateral redistribution as a result of fluctuations in the microscopic interactions between individual components (22). Similar organizational energetics have previously been shown to be exhibited by a variety of model membrane bilayer mixtures (21, 23, 24). The resultant concentration profiles illustrated the existence of a significant P dependence in the ensemble transfer of excited state energy between fluorophore molecules and was greatest for $\overline{R}_0/L$ values $\simeq 1$.

The numerical techniques presented in this communication provide a theoretical basis through which P values may be calculated for a variety of membrane bilayer systems. These determinations require only that the value of $\overline{R}_0/L$ and the molar concentration of fluorescent species be known. For near random distributions of fluorophores, the quenching profiles for experimental probe concentrations (0.5–5.0 mol %) were shown to be relatively independent of the distance of closest approach between fluorescent molecules. For the continuous space, this result is expected to hold true, due to a local disorder of the molecular packing, even for fluorescent systems exhibiting significant amounts of lateral species separation. Thus, for a large number of experimental systems, the determination of P may not require that the minimum separation between molecular constituents be known exactly. In this way, the energetic interaction between selected components may be calculated solely from the observed transfer efficiencies and normalized acceptor concentrations.

As a specific application, the quenching properties of fluorescent systems containing a mixture of donor and acceptor species, each with unique distribution characteristics, were investigated. It was found that the existence of phase-separated domains of protein or lipid molecules to which donor fluorophores are covalently linked gives rise to a shielding effect such that donor and acceptor moieties are isolated from one another and relative transfer efficiencies are decreased. Increased concentrations of the phase-separated component or increased ratios $\overline{R}_0/L$ were found to enhance this organizational effect. These results illustrate the existence of a significant P dependence in the transfer of excited state energy between respective components in both protein-lipid and lipid-lipid bilayer mixtures. As such, the results from the present numerical method suggest that the experimental application of quenching measurements to these membrane systems will permit a precise determination of specific organizational parameters within the bilayer. Furthermore, for large values of $\overline{R}_0/L$ and a radially displaced donor fluorophore with random angular orientation, the resulting quenching curves were found to be ensemble averaged, yielding profiles identical to those calculated with a center of mass donor placement. Thus, for membrane systems whose rotational degrees of freedom are unrestricted, an accurate determination of lateral donor positioning (e.g., within complex intramembraneous proteins) will in principle not be required because the fluorophore moieties can be assumed to be centrally located within the host molecule.

The uncertainty involved in a calculation of the types described above (i.e., the intrinsic error involved in an experimental evaluation of $\overline{R}_0$) is primarily determined by the relative dipole orientations of the donor and acceptor excitons (6). For most cases, the relative orientations are assumed to be isotropic with dynamic averaging over the lifetime of the donor excitation. This yields an average orientation factor $\langle \kappa^2 \rangle$, proportional to $\overline{R}_0$, of 2/3. If the isotropic condition is not satisfied, however, upper and lower bounds for $\langle \kappa^2 \rangle$ can be estimated from the dynamic relaxations of the respective dipole orientations and these limits may be further reduced if the transfer depolarization between donor and acceptor pairs is known (28). For applications such as those presented in this chapter, the calculated error in $\langle \kappa^2 \rangle$, and hence $\overline{R}_0$, is normally less than $\pm 10\%$.

Although the present study has centered on two-dimensional binary mixtures in which molecular dynamics are neglected, the simulative nature of the method will permit an uncomplicated extension to more complex membrane systems. For example, organizational parameters may similarly be obtained for molecules to which the fluorescent moieties are covalently linked or for compositional domains for which the fluorescent species exhibit a preferential affinity. In addition, the generation technique may be modified in a straightforward manner to take into account the depth within the bilayer, full or partial constraint of the respective dipole orientations of the fluorophore molecules, and rotational or translational diffusion within the bilayer. Thus, in principle, this approach is not limited or constrained by the diversity of a particular bilayer system and hence can be considered directly applicable for organizational determinations in biological membranes.

In this study, a static Monte Carlo technique has been applied to the problem of fluorescence energy transfer in

two dimensions to provide a quantitative measure of the effects of excluded volume interactions, specific lattice structures, and nonrandomness in the mixing of fluorescent species on expected quenching and depolarization efficiencies. These results provide a generalized exact solution for the concentration dependence of the transfer of both polarized and unpolarized excited state radiation for fluorescent systems exhibiting either unidirectional or reciprocal energy transfer.

The authors thank Dr. A. M. Kleinfeld for many helpful discussions.

Supported by grants GM-30819 and GM-26894 from the National Institutes of Health

Received for publication 14 January 1982 and in revised form 20 May 1982.

REFERENCES

1. Stryer, L. 1978. Fluorescence energy transfer as a spectroscopic ruler. *Annu. Rev. Biochem.* 47:819–846.
2. Veatch, W., and L. Stryer. 1977. The dimeric nature of the gramicidin A transmembrane channel: conductance and fluorescence energy transfer studies of hybrid channels. *J. Mol. Biol.* 113:89–102.
3. Hahn, L. H. E., and G. G. Hammes. 1978. Structural mapping of aspartate transcarbamoylase by fluorescence energy transfer measurements: determination of the distance between catalytic sites of different subunits. *Biochemistry.* 17:2423–2429.
4. Koppel, D. E., P. J. Fleming, and P. Strittmatter. 1979. Intramembrane positions of membrane-bound chromophores determined by excitation energy transfer. *Biochemistry.* 18:5450–5457.
5. Lee, A. G. 1975. Segregation of chlorophyll *a* incorporated into lipid bilayers. *Biochemistry.* 20:4397–4402.
6. Fung, B. K.-K., and L. Stryer. 1978. Surface density determination in membranes by fluorescence energy transfer. *Biochemistry.* 17:5241–5248.
7. Rogers, J., A. G. Lee, and D. C. Wilton. 1979. The organisation of cholesterol and ergosterol in lipid bilayers based on studies using nonperturbing fluorescent sterol probes. *Biochim. Biophys. Acta.* 552:23–37.
8. Kimelman, D., E. S. Tecoma, P. K. Wolber, B. S. Hudson, W. T. Wickner, and R. D. Simoni. 1979. Protein-lipid interactions. Studies of M13 coat protein in dimyristoylphosphatidylcholine vesicles using paranaric acid. *Biochemistry.* 18:5874–5880.
9. Knox, R. S. 1968. Theory of polarization quenching by excitation transfer. *Physica (Utrecht).* 39:361–386.
10. Weber, G. 1960. Fluorescence-polarization spectrum and electronic-energy transfer in tyrosine, tryptophan and related compounds. *Biochem. J.* 75:335.
11. Weber, G., and E. Daniel. 1966. Cooperative effect in the binding on bovine serum albumin II. The binding of l-anilino-8-naphtalenesulfanate. Polarization of the ligand fluorescence and quenching of the protein fluorescence. *Biochemistry.* 5:1900.
12. Kelly, A. R., and L. K. Patterson. 1971. Model systems for photosynthesis II. Concentration quenching of chlorophyll fluorescence in solid solutions. *Proc. R. Soc. Ser. A.* 324:117–126.
13. Dissing, S., A. J. Jesaitis, and P. A. G. Föortes. 1979. Fluorescence labeling of the human erythrocyte anion transport system. Subunit structure studied with energy transfer. *Biochim. Biophys. Acta.* 553:66–83.
14. Förster, T. 1949. Experimentelle and theoretische Untersuchung des zwischenmolekuaren Übergans von Elektronenanregungsenergie. *A. Naturforsch. A. Astrophys. Phys. Chem.* 4:321.
15. Ore, A. 1959. Intermolecular energy transfer and concentration depolarization of fluorescent light. *J. Chem. Phys.* 31:442.
16. Weber, G. 1954. Dependence of the polarization of the fluorescence on the concentration. *Trans. Faraday Soc.* 50:552.
17. Craver, F. W., and R. S. Knox. 1971. Theory of polarization quenching by excitation transfer II. Anisotropy and second-neighbor considerations. *Mol. Phys.* 22:385–402.
18. Craver, F. W. 1971. Theory of concentration quenching of fluorescence polarization in two-dimensional solutions. *Mol. Phys.* 22:403–420.
19. Wolber, P. K., and B. S. Hudson. 1979. An analytic solution to the Förster energy transfer problem in two dimensions. *Biophys. J.* 28:197–210.
20. Dewey, T. G., and G. G. Hammes. 1980. Calculation of fluorescence resonance energy transfer on surfaces. *Biophys. J.* 32:1023–1035.
21. Freire, E., and B. Snyder. 1980. Estimation of the lateral distribution of molecules in two-component lipid bilayers. *Biochemistry.* 19:88–94.
22. Freire, E., and B. Snyder. 1980. Monte Carlo studies of the lateral organization of molecules in two-component lipid bilayers. *Biochim. Biophys. Acta.* 600:643–654.
23. Snyder, B., and E. Freire. 1980. Compositional domain structure in phosphatidylcholine-cholesterol and sphingmyelin-cholesterol bilayers. *Proc. Natl. Acad. Sci. U. S. A.* 77:4055–4059.
24. Freire, E., and B. Snyder. 1982. Quantitative characterization of the lateral distribution of membrane proteins within the lipid bilayer. *Biophys. J.* 37:617–624.
25. Dexter, D. L. 1953. A theory of sensitized luminescence in solids. *J. Chem. Phys.* 21:836.
26. Montroll, E. W., and K. E. Schuler. 1958. The application of the theory of stochastic processes to chemical kinetics. *Adv. Chem. Phys.* 1:361.
27. Knox, R. S. 1968. On the theory of excitation in the photosynthetic unit. *J. Theor. Biol.* 21:244–259.
28. Dale, R. E., J. Eisinger, and W. E. Blumber. 1979. The orientational freedom of molecular probes: the orientation factor in intramolecular energy transfer. *Biophys. J.* 26:161–193.